Supplemental Information

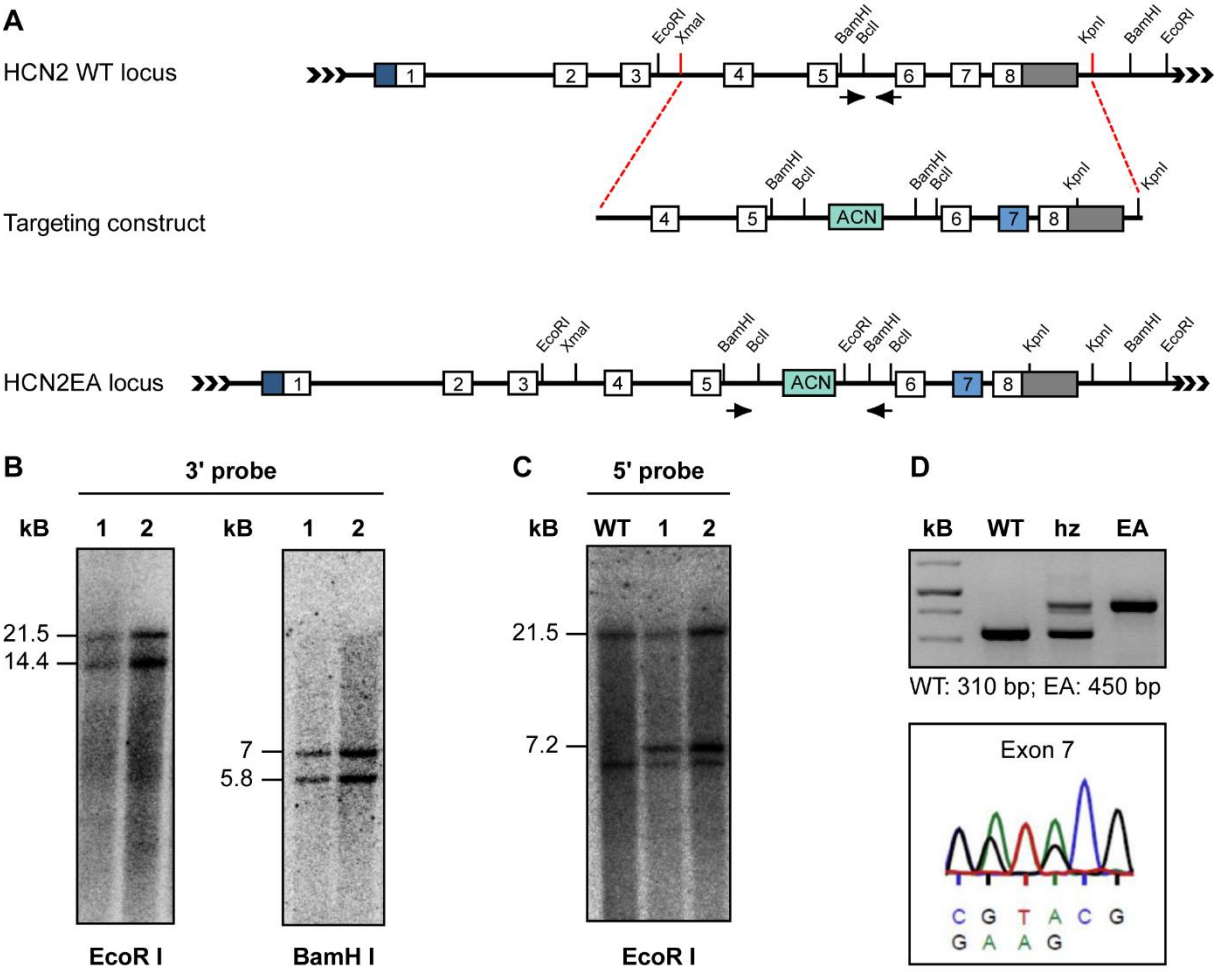

Supplemental Figure 1. Generation of the HCN2EA mouse model. **(A)** Top: wild-type HCN2 locus and targeting vector. Exons 1-8 are indicated by open boxes. The targeting vector contains an ACN self-excision neomycine resistance cassette (54) (green) and carries point mutations in exon 4 (marked in blue) to generate the R591E, T592A exchanges. Bottom: knockin HCN2EA allele obtained after homologous recombination in ES cells **(B)** Southern Blots showing the correct 3' integration of the targeting construct. **(C)** Southern Blots showing the correct 5' integration of the targeting construct. **(D)** Genotyping results of WT, heterozygous and HCN2EA mice (upper panel). The locations of the sense and antisense primer are indicated as small arrows in S1a. Electropherogram of the mutated base pairs in exon 7 in heterozygous mice (lower panel). See Methods for primer sequences.

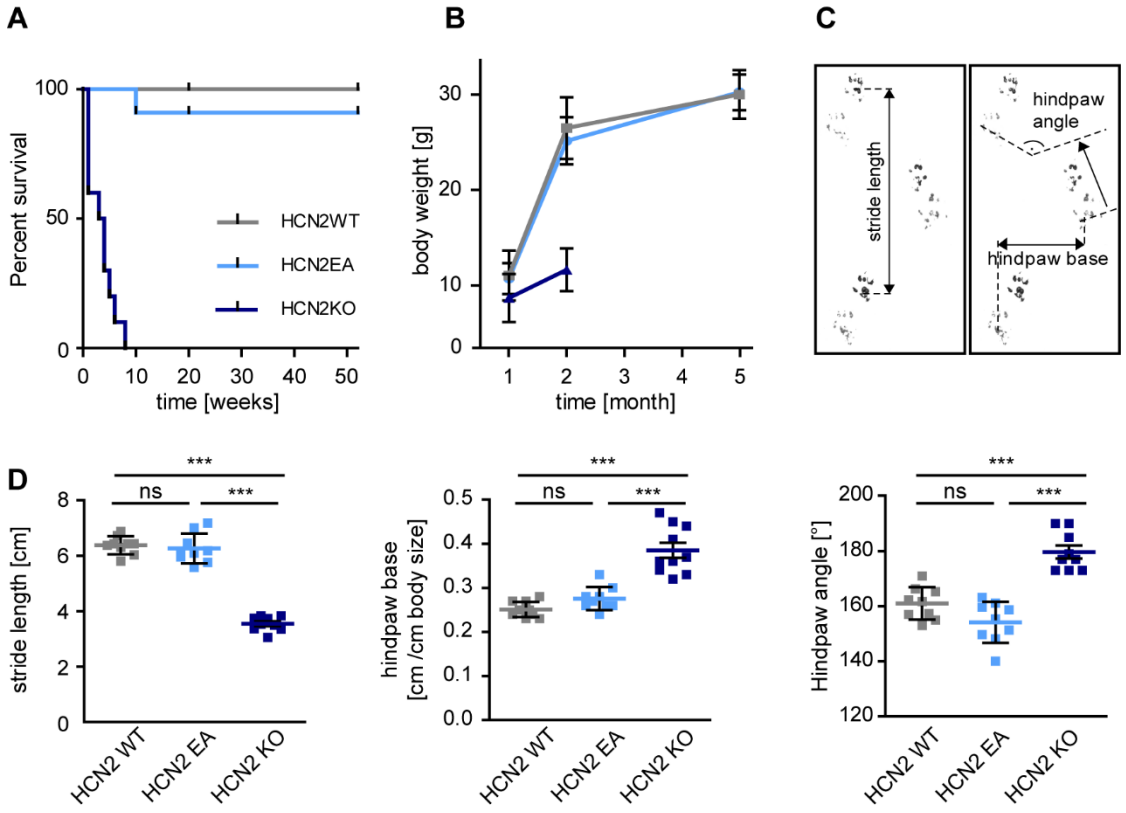

Supplemental Figure 2. Phenotype of the HCN2EA mouse. **(A)** Meier-Kaplan blot of WT (gray, n=16), HCN2EA littermates (light blue, n=16) and HCN2 KO mice (dark blue, n=10). **(B)** Body weight of WT (gray, n=33), HCN2EA littermates (light blue, n=31) and HCN2 KO mice (dark blue, n=18) over time. **(C)** Example of a footprint analysis showing stride length, hindpaw angle and hindpaw base. **(D)** Stride length (left panel), hindpaw base (middle panel) and hindpaw angle (right panel) of WT (gray) and HCN2EA littermates (light blue) and HCN2 KO mice (dark blue) (WT: n=8, HCN2EA: n=9, HCN2 KO: n=10; One-Way ANOVA, Bonferroni's post hoc test).

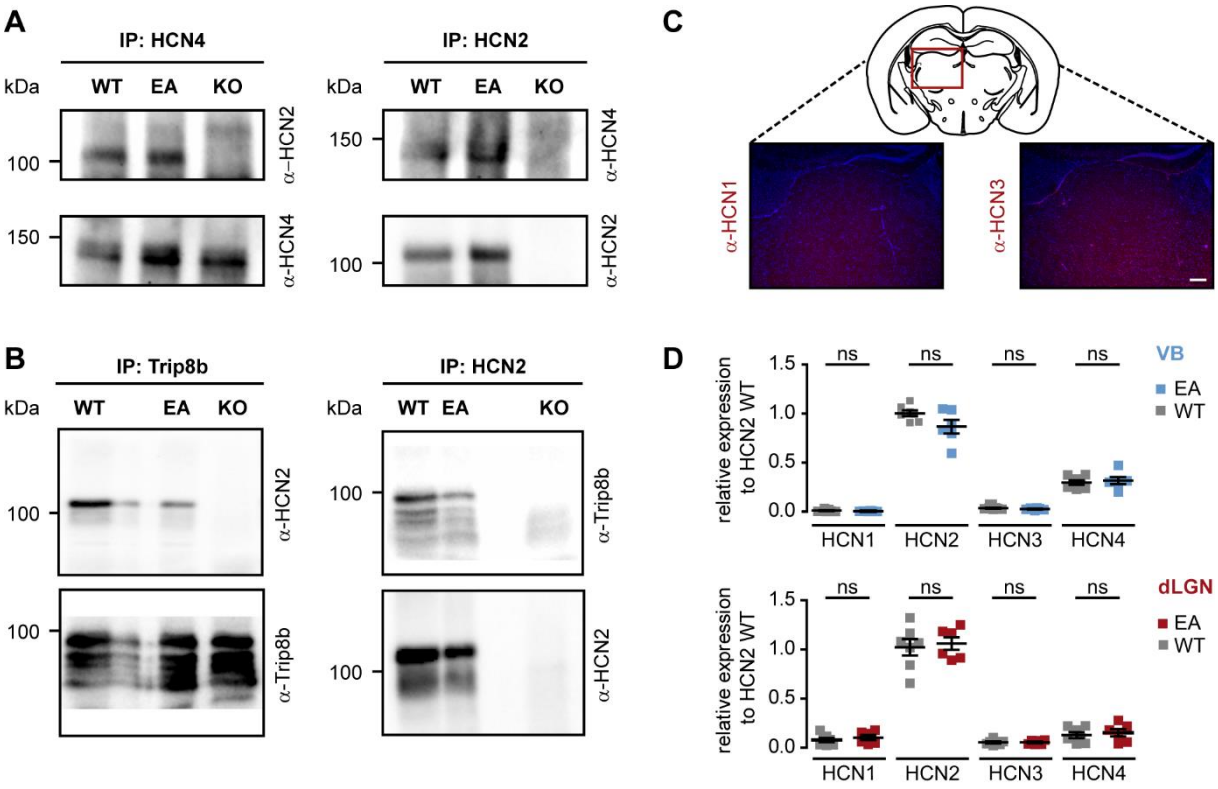

Supplemental Figure 3. Interaction and localization of HCN channels in the brain. **(A)** Co-Immunoprecipitations of lysates of whole WT brain (left lanes), HCN2EA (middle lanes) and HCN2-KO (right lanes), precipitated either with anti-HCN2 (alomone) or anti-HCN4 (alomone). **(B)** Co-Immunoprecipitations of lysates of whole WT brain (left lanes), HCN2EA (middle lanes) and HCN2-KO (right lanes), precipitated either with anti-Trip8b (alomone) or anti-HCN2 (alomone). **(C)** Immunostainings for HCN1 and HCN3 in coronal brain slices of the thalamus (as marked by the red square in the scheme of the mouse brain). Specific immunosignal is in red. Nuclei have been counterstained with Hoechst (blue), scale 200 µm. **(D)** Lack of cAMP modulation in HCN2 does not alter the expression level of HCN isoforms in VB and dLGN in WT and HCN2EA mice. The expression levels of HCN isoforms are shown for the VB (upper) and dLGN (lower panel) in WT (gray, n=7) and HCN2EA mice (blue (VB) and red (dLGN), n=6). One-Way ANOVA, Bonferroni's post hoc test showed no significant diffenrence between WT and HCN2EA.

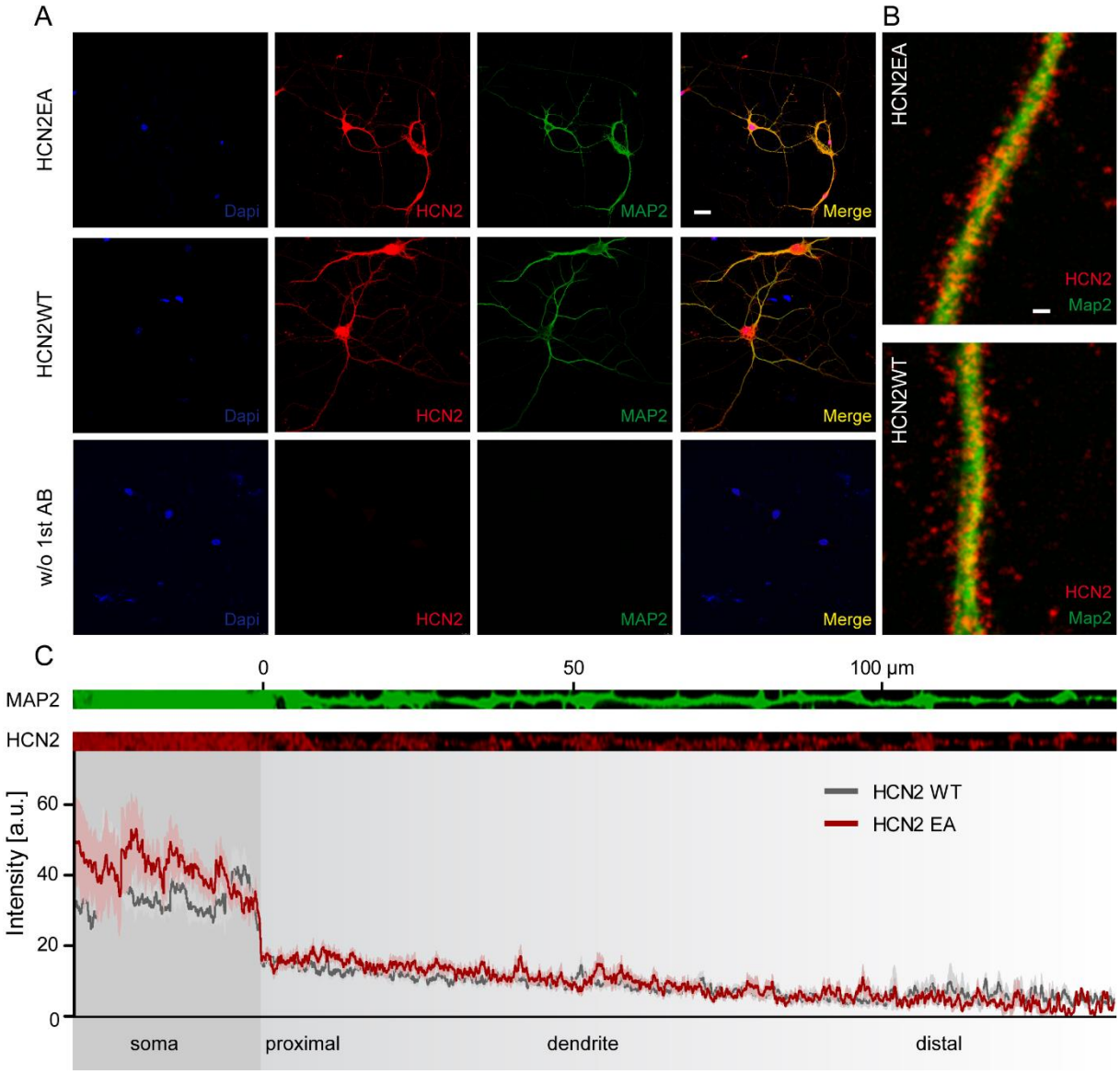

Supplemental Figure 4. Localization of HCN2 channels in soma and dendrites of primary neurons. **(A)** Primary hippocampal neurons of P0 HCN2EA or HCN2WT mice were transfected with either HCN2EA (upper) or HCN2WT DNA (middle panel). Neurons were stained at DIV14 for cell nuclei (Dapi; blue), HCN2 (α-HCN2; red) and dendrites (α-MAP2; green). Merged pictures show colocalization of HCN2 and MAP2 in the dendrites of primary neurons. Negative control (lower panel) showed specificity of the antibodies used. Scale: 20 µm. Representative primary neuron of cells analyzed in (C). **(B)** High-resolution images of dendrites shown in (A) revealed HCN2 staining at dendritic spines. Scale: 3 µm **(C)** Dendrites were identified using MAP2 (upper panel, green) and the intensity of HCN2 (middle panel; red) was measured using the Plot Profile Plugin (ImageJ). The intensity was plotted against the distance from the soma for WT (grey; n=17) and the HCN2EA mutant (red; n=16) (lower panel) and revealed no difference in the expression along dendrites and somata.

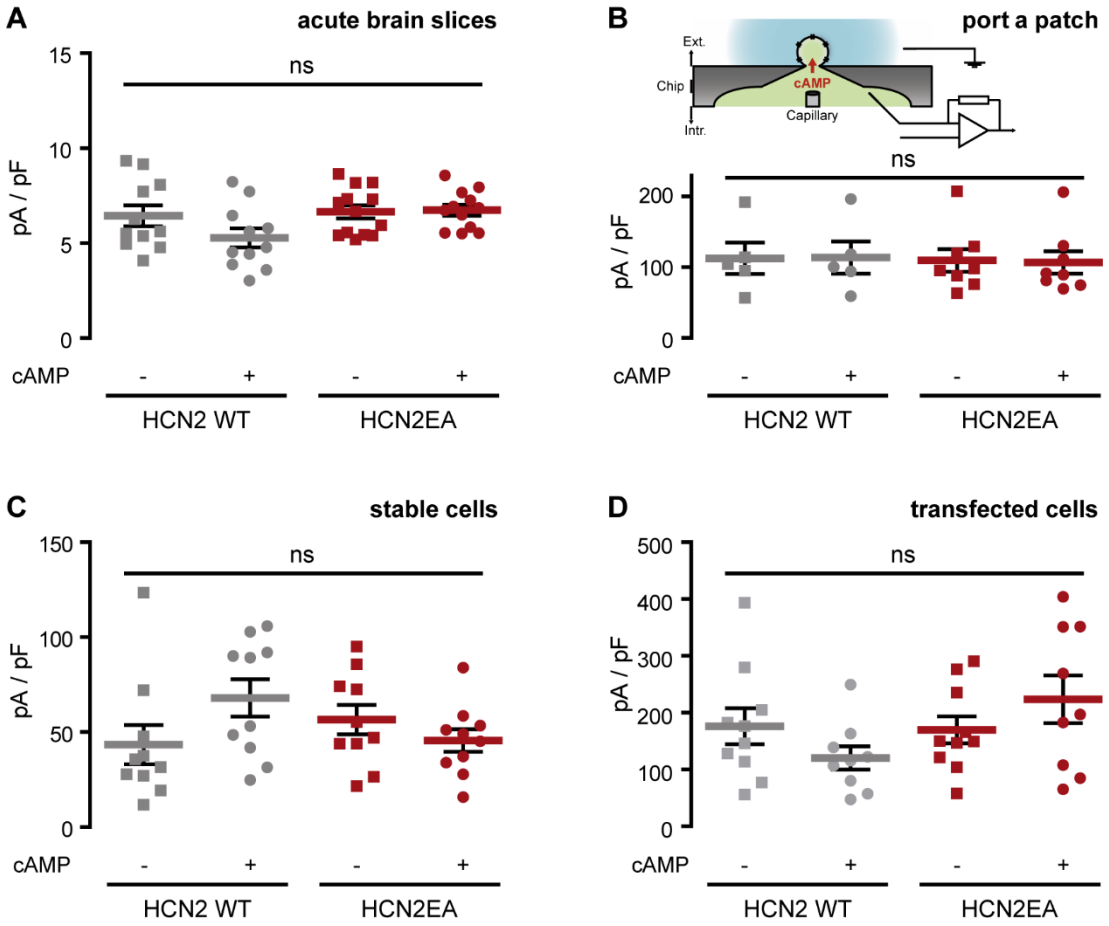

Supplemental Figure 5. (A) Current densities in acute brain slices. WT (gray squares: -cAMP, n=11; gray circles: +cAMP, n=11), HCN2EA (red squares: -cAMP, n=13; red circles: +cAMP, n=12). **(B)** Current densities in internally perfused cells using the port-a-patch system**.** WT (gray squares: -cAMP, n=5; gray circles: +cAMP, n=5), HCN2EA (red squares: -cAMP, n=8; red circles: +cAMP, n=8). **(C)** Current densities in stable HEK293 cells. WT (gray squares: -cAMP, n=10; gray circles: +cAMP, n=11), HCN2EA (red squares: -cAMP, n=10; red circles: +cAMP, n=10). **(D)** Current densities in transfected HEK293 cells. WT (gray squares: -cAMP, n=10; gray circles: +cAMP, n=9), HCN2EA (red squares: -cAMP, n=10; red circles: +cAMP, n=9). WT HCN2 current densities (gray) were compared to HCN2EA current densities (red) in absence (squares) and presence (circles) of cAMP (One-way ANOVA; Bonferroni post-hoc test).

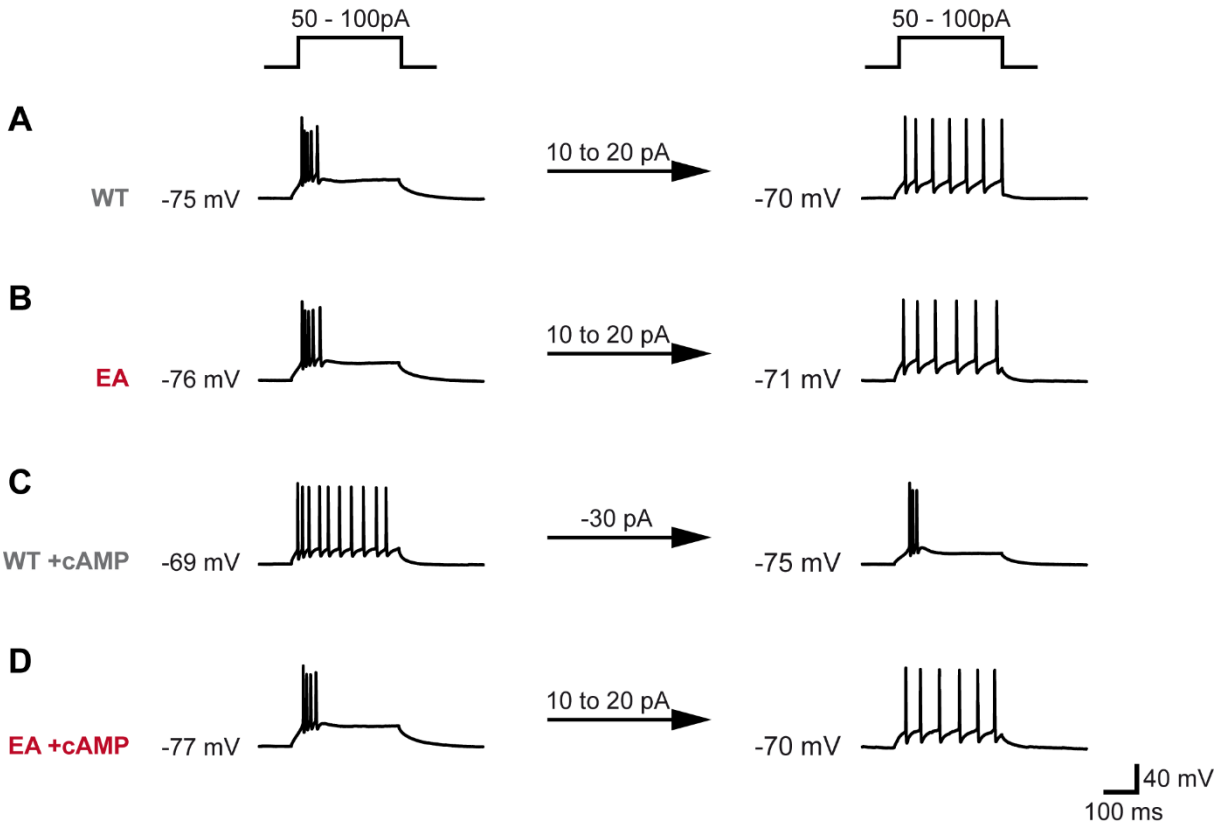

Supplemental Figure 6. Firing modes depend on the membrane potential. Shown are firing patterns elicited by 300 ms depolarizing current steps of 50 or 100 pA. Without cAMP, WT **(A)** and EA **(B)** neurons fire in burst mode when depolarized from their RMP. When bringing the membrane potential to higher values by constant current injection of 10-20 pA, cells show tonic firing upon step current injections. Application of cAMP in WT **(C)** and EA **(D)** neurons leads to different RMPs (-69 mV and -77 mV, respectively). Depolarizing step current injections elicit different responses in WT + cAMP (tonic, C) and EA + cAMP (burst, D) neurons. Constant negative current injections brings the membrane potential of WT + cAMP to a more negative value and step current injections applied thereafter lead to these cells firing in burst mode (C). Vice versa, the membrane potential of EA + cAMP neurons was elevated to a more positive value by constant current injections of 10-20 pA and step current injections now elicit tonic firing (D).. Shown are representative traces (WT: n = 6, HCN2EA: n = 7, WT + cAMP: n = 4, HCN2EA + cAMP: n = 7).

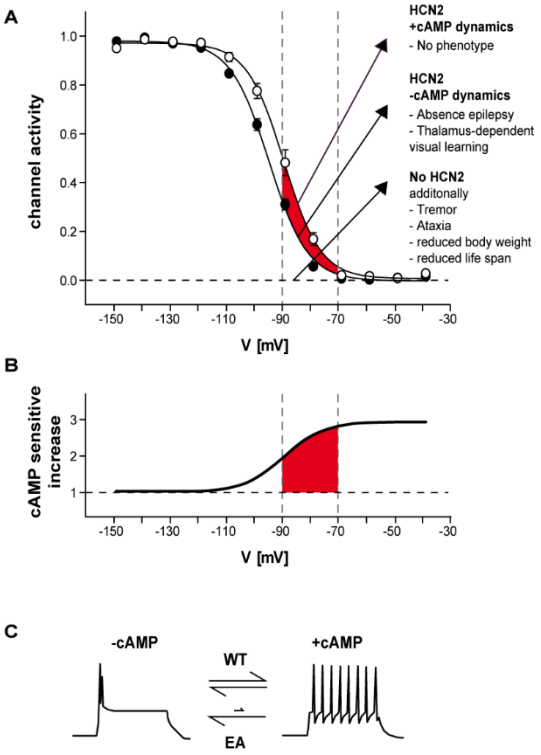

Supplemental Figure 7. Model for the physiological role of cAMP-sensitive modulation of HCN2 on the level of the channel, at the level of the cell and the in vivo level. **(A)** Cartoon for the steady state activation curve of HCN2 in the absence (closed circles) and presence (open circles) of intracellular cAMP in TC neurons. The physiological range of membrane potentials is indicated by vertical broken lines (-90 mV to -70 mV). In the absence of cAMP, only a fixed amount of channel activity is available in wild type HCN2 channels (steady state activation curve on the left). On top, a cAMP-sensitive proportion of channel activity of wild-type HCN2 can be gradually tuned according to cellular needs by cAMP. The red region indicates the dynamic range of channel activity, which can be recruited by cAMP. HCN2EA channels cannot bind cAMP and, hence, are unresponsive to changes in the cAMP concentration. Right panel: phenotypes which correspond to individual regions **(B)** from steady state activation curves shown in panel (a), cAMP-sensitive increase in the presence of cAMP as compared to control conditions without cAMP is calculated as I_{+cAMP}/I_{-cAMP}. The red region indicates the dynamic range of cAMP sensitive increase in channel activity. **(C)** Cartoon of typical burst firing in the absence of cAMP (left) and tonic firing in the presence of cAMP (right) for TC neurons of WT mice. In these neurons, increase and decrease in intracellular cAMP can switch between these firing modes. In contrast, TC neurons of HCN2EA mice are less likely to switch from burst to tonic firing in response to cAMP and rather stably remain in the burst firing mode.